

Interplay of collisions with quasilinear growth rates of relativistic electron-beam-driven instabilities in a superdense plasma

C. Deutsch

L.P.G.P. (CNRS-UMR-8578) Bât. 210, UPS, 91405 ORSAY Cedex, France

A. Bret

ETSI Industriales, Universidad de Castilla-La Mancha, 13071 CIUDA REAL, Spain

M.-C. Firpo

L.P.T.P. (CNRS-UMR-7648), Ecole Polytechnique, 91118 PALAISEAU Cedex, France

P. Fromy

CRI, Bât. 210, UPS 91405 ORSAY Cedex, France

(Received 28 December 2004; published 3 August 2005)

We focus attention on the rapidly growing electromagnetic instabilities arising in the interaction of intense and relativistic electron beams (REB) with supercompressed thermonuclear fuel. REB-target system is considered neutralized in charge and current with a distribution function including beam and target temperatures. The electromagnetic filamentation (Weibel) instability is first considered analytically in a linear approximation. Relevant growth rates parameters then highlight density ratios between target and particle beams, as well as transverse temperatures. Significant refinements include mode-mode coupling and collisions with target electrons. The former qualify the so-called quasilinear (weakly turbulent) approach. Usually, it produces significantly lower growth rates than the linear ones. Collisions enhance them slightly for $kc/\omega_p < 1$, and dampen them strongly for $kc/\omega_p \geq 1$. In a low temperature target plasma, intrabeam scattering also contributes to the instability taming, while keeping it close to zero in a warm plasma. Our numerical exploration provides further support to the cone-angle configuration (Osaka experiment) with REB penetrating close to the dense core of superdense deuterium+tritium fuel.

DOI: [10.1103/PhysRevE.72.026402](https://doi.org/10.1103/PhysRevE.72.026402)

PACS number(s): 52.35.Qz, 52.35.Hr, 52.50.Gj, 52.57.Kk

I. INTRODUCTION

One can still notice a rather high level of current interest for the interaction physics of intense and relativistic electron beams (REB) with superdense deuterium+tritium (DT) plasmas. Corresponding target electron n_p density ranges between 10^{23} electrons/cm³ for the outer layer of compressed DT core (see Fig. 1) and 10^{26} electrons/cm³ at center. Such a concern is basically motivated by the fast ignition scenario (FIS) for inertial confinement fusion (ICF) driven by intense and laser produced REB with number density $n_b \sim 10^{22}$ electrons/cm³ [1]. Such a scheme outlines to the extreme the separation of compression driven by lasers, heavy ion beams or Z pinches, from the controlled ignition through REB which thus relieves to a large extent the energy request on initial precompression. The successful completion of such an approach to ICF demands a careful control of any electromagnetic instability susceptible to evolve very swiftly within the REB-target system. Such an instability is potentially able to divert transversally with respect to initial REB propagation, and nearly instantaneously, a significant amount of the incoming REB translation energy.

That process is not only quantitative, it is also highly likely to occur through a filamentation with a substantial degradation of beam focusing capabilities.

Such concerns are by no means restricted to ICF physics. They also play a central role in solar flares [2], for instance,

as well as in some laboratory plasmas where filamentation (Weibel) instabilities could be seen degraded into highly nonlinear Langmuir turbulence [3].

Recently, our group has devoted a very thorough scrutiny to the interplay of filamentation (Weibel) electromagnetic instabilities with the more mundane two-stream and longitudinal instability [4]. As a result, a previously unnoticed oblique ridge has thus been unravelled in the space delimited by the growth rate and the two corresponding wavenumber coordinates. However, those studies are still restricted to a collisionless situation. Here, we do focus attention on the so-called filamentation (Weibel) branch identified in these

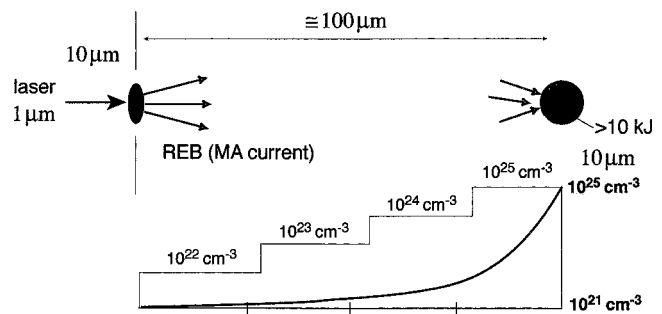


FIG. 1. Relativistic electron beam (REB) propagation with MeV incoming energy through layers of increasing density N_p in a core of precompressed DT fuel.

preliminary investigations [4]. A complete exploration, including collisions with two-stream altogether, is postponed to further inquiries.

Here, we intend to focus attentions on the very large densities implied in a realistic beam-target interaction of FIS interest [1,5,6]. Despite that beam particle density n_b always fulfills a weak beam approximation $n_b \ll n_p$, it should be taken around $n_b \sim 10^{22}$ electrons/cm³ to secure on a 10 nsec time scale several tens of kJ to the off-center hot spot requested for DT ignition. Such a situation implies that the usual collisionless assumption used in working out electromagnetic instabilities through the Vlasov equation be removed. At this juncture, a few earlier endeavors dedicated to the interplay of electromagnetic instabilities with electron-electron collisions should be recalled [7–9]. Okada and Niu [7] make use of a Vlasov framework and characterize the beam-plasma interaction with an anisotropic superposition of Maxwell distributions. These authors were concerned by an earlier ICF approach based on the use of intense REB for compressing directly DT fuels. In the meantime, this approach has been recognized as impractical, in view of the rapid growth of transverse hydrodynamical instabilities [10] severely limiting the increase in target density.

However, the given beam-target modeling is easily transferable to FIS of a precompressed DT target, thus avoiding the former and unfortunate hydroexpansion effect. Later on, Wallace *et al.* [8] used the Los Alamos Venus code to document the effect of e - i and e - e Rutherford scattering collisions in target on the Weibel growth rate in a laser produced plasma. They noticed that the Weibel mechanism is not severely altered by the presence of collisions. It is seen simply weakened as collisionality is increased. It should also be mentioned that the given target plasma parameters are very different from the FIS ones, and the filamentation instability is not REB driven, in this case.

Much more recently, Krueer *et al.* [9] have presented 2D and 3D particle-in-cell (PIC) simulations for REB-plasma interaction of FIS relevance. They also notice a weakening of Weibel growth rates when collisions are included.

As far as we know, all those works considered electron-electron (e - e) and electron-ion (e - i) collisions in target. We will demonstrate in the latter that for the very dense REB considered in fast ignition, intrabeam scattering may also play a significant role. Same remarks also apply to the very recent and linear analysis displayed by Honda [11], who extends to e - e collisions and FIS parameters, former extensive and collisionless investigations of electromagnetic instabilities in astrophysical plasmas by the Pisa Group [12–14].

Honda [11] displays an extensive eigenmodes study and come up with filamentation growth rates which tend to saturate when $kc/\omega_p \sim 1$ in terms of the target electron plasma frequency ω_p . We do agree in the sequel with this conclusion. However, these collisional and linear growth rates are still too large to be of practical use in the FIS modus operandi.

This explains that we give also attention to quasilinear growth which retain the effect of *in situ* electromagnetic fields on target particle trajectories.

In the sequel, we shall often refer to the filamentation (Weibel) instability as the Weibel electromagnetic instability (WEI) [15].

At this juncture, it should be appreciated that present emphasis on linear and quasilinear approach is not only motivated by analytic tractability. It is also a genuine basic concern to understand quantitatively the WEI onset at its earlier beginning when it is competing with the REB energy loss through electron-electron collisions. This kind of information is rather difficult to unravel from 3D particle-in-cell (PIC) codes, in view of their intrinsic numerical noise [16], which often lends them to skip too swiftly the crucial and initial linear stage, while jumping directly into the fully nonlinear one.

FIS demands on filamentation (Weibel) growth rates are displayed in Sec. II. Okada-Niu formalism [7] for the REB-target interaction with collision included is adapted to the fast ignitor scheme in Sec. III. We thus stress the pivotal significance of asymmetry parameters for beam and target plasmas, respectively. Quasilinear improvements are detailed in Sec. IV, within a Dupree-Weinstock approach [17] conveniently rephrased by Kono and Ichikawa [18]. Section V displays the resulting growth rate profiles through a rather extensive parameter study. Conclusions are offered in Sec. VI.

II. FIS CONSTRAINTS ON WEI GROWTH RATES

In order to get the femtolaser produced REB through the huge density gradient (see Fig. 1) of compressed fuel, the relativistic electrons should experience only a small energy loss in the less dense outer layers. The corresponding REB should thus keep, as much as possible, its emittance unperturbed before reaching the most dense region.

The most deleterious effect which could prevent an efficient REB penetration toward dense fuel core is featured by the WEI able to divert swiftly and transversally to initial REB orientation a significant fraction of its kinetic energy. So, a crucial figure of merit is the number of WEI e -foldings

$$N_{e\text{-fold}} = \delta_{\max} T_{\text{stop}}, \quad (1)$$

in terms of REB relativistic stopping time ($\beta_b = v_b/c$)

$$T_{\text{stop}} = \frac{1}{c} \int_{E_b^{\min}}^{E_b^{\max}} \frac{1 + \frac{E_b}{m_e c^2}}{\left[\left(\frac{E_b}{m_e c^2} \right) \left(\frac{E_b}{m_e c^2} + 2 \right) \right]^{1/2}} \frac{dE_b}{dx}, \quad (2)$$

$$\cong \frac{100}{4} \times 10^{-4} \text{ cm} \times \frac{1}{\beta_b c \text{ cm/sec}}$$

$$\cong 10^{-13} \text{ sec} \quad \text{for 1 MeV REB}$$

travelling through 25 μm of constant density plasma target.

In the collisionless regime, WEI has received a number of extensive treatments [19–23], in various plasma configurations, with or without impinging particle beams. In particular, Davidson *et al.* [21] devoted a lot of attention to beam-target interaction monitored by a constant and axial magnetic field.

III. LINEAR TREATMENTS

Here we follow quite closely an earlier and very clear presentation of Okada and Niu [7]. REB and target plasma are taken initially unmagnetized, with immobile target ions. The latter have a typical plasma frequency much lower than that of the electrons, which monitor the growth rate time scale. The incoming beam is considered, homogenous and spatially infinite.

Beam-target system is taken neutral. REB propagates with overall velocity \vec{v}_d^b . As in Ref. [7], we focus on an electromagnetic mode with wave number \vec{k} orthogonal to \vec{v}_d^b , perturbed electric field $\vec{E} \parallel \vec{V}_d^b$ and perturbed magnetic field \vec{B} normal to \vec{v}_d^b and \vec{E} . This choice stands at variance with the Honda linear analysis [11] based also on a purely transverse mode with $\vec{k} \perp \vec{V}_d^b$, but with $\vec{B} \parallel \vec{V}_d^b$ and \vec{E} normal to \vec{k} and \vec{B} .

Beam-target interaction is considered in a weak beam approximation with a ratio of target electron density n_p to beam density n_b , $r = n_b/n_p \ll 1$, in full agreement with FIS prescriptions. Presently, we characterize the beam and target electrons, respectively, with a classical Fried-Conte [24] dielectric function,

$$W(z) = \lim_{\nu \rightarrow 0^+} (2\pi)^{-1/2} \int_{-\infty}^{\infty} \frac{y}{y - z - i\nu} \exp\left(-\frac{1}{2}y^2\right) dy. \quad (3)$$

In the near future we also intend to include partial degeneracy [25] effects required in a low temperature precompressed DT plasma.

According to Ref. [7] (Okada-Niu) we now model the REB-target electron interaction with equilibrium bi-Maxwellian distribution

$$f_0(\mathbf{p}) = \frac{n_p}{2\pi m (\theta_x^p \theta_y^p)^{1/2}} \exp\left(-\frac{(p_x + p_d^p)^2}{2m\theta_x^p} - \frac{p_y^2}{2m\theta_y^p}\right) + \frac{n_b}{2\pi m \gamma_b (\theta_x^b \theta_y^b)^{1/2}} \exp\left(-\frac{(p_x + p_d^b)^2}{2m\gamma_b \theta_x^b} - \frac{p_y^2}{2m\gamma_b \theta_y^b}\right). \quad (4)$$

Here θ_x, θ_y are the temperature components parallel to the x and y directions, p_d is the drift momentum, and superscripts p and b represent the plasma electron and the beam electron, respectively. The linearized Vlasov equation reads as

$$\frac{\partial f}{\partial t} + \mathbf{v} \cdot \frac{\partial f}{\partial \mathbf{r}} + q \left(\mathbf{E} + \frac{\mathbf{v}}{c} \times \mathbf{B} \right) \cdot \frac{\partial f}{\partial \mathbf{p}} = -\nu(f - f_0), \quad (5)$$

where ν is the effective collision frequency, to be precised latter, f is the electron distribution function at position \mathbf{r} and momentum \mathbf{p} at time t , f_0 is the equilibrium distribution function, q denotes the electric charge (including sign), c is the velocity of light \mathbf{v} and \mathbf{p} are related by $\mathbf{v} = \mathbf{p}/m\gamma_b$, $\gamma_b = [1 + p^2/(mc)^2]^{1/2}$ and m is the electron rest mass.

From Eqs. (4) and (5) one easily obtains through a well-known and simultaneous linearization of Vlasov Eq. (5) and Maxwell equations, linear dispersion relations for purely transverse modes with respect to initial beam orientation. Standard procedures based in linear susceptibilities χ_p^L for the

target plasma and χ_b^L for the beam plasma allow to put the linear dispersion relation for a purely transverse mode under the form

$$1 + \chi_p^L(k, \omega) + \chi_b^L(k, \omega) = k^2 c^2 / \omega^2, \quad (6)$$

$$\chi_p^L(k, \omega) = \frac{\omega_p^2}{\omega(\omega + i\nu)} \left[1 - \text{AW}(\xi) - \frac{i\nu}{\omega} (A - 1) W(\xi) \right], \quad (7)$$

$$\chi_b^L(k, \omega) = \frac{\omega_b^2}{\omega^2} [1 - \text{BW}(\eta)], \quad (8)$$

where

$$\omega_p^2 = \frac{4\pi n_p e^2}{m}, \quad \omega_b^2 = \frac{4\pi n_b e^2}{m\gamma_b}, \quad (9a)$$

$$A = (\theta_x^p + p_d^{p2}/m)/\theta_y^p, \quad B = (\theta_x^b + p_d^{b2}/m\gamma_b), \quad (9b)$$

$$\xi = \frac{(\omega + i\nu_p)}{k(\theta_y^p/m)^{1/2}}, \quad \eta = \frac{(\omega + i\nu_b)}{k(\theta_y^b/m\gamma_b)^{1/2}}, \quad (9c)$$

γ_b denotes the usual Lorentz factor $[1 - (v_b^2/c^2)]^{-1/2}$ for a monochromatic beam.

In contradistinction to many earlier works, the very high beam density ($n_b \sim 10^{22}$ electrons/cm³) indulges us in assigning a collision frequency ν_b to the incoming REB plasma. Let us also notice that η [Eq. (9c)] is normalized by a nonrelativistic thermal velocity with a γ_b factor.

This is correct in the limiting cases $\gamma_b = 1$ (nonrelativistic) and $\gamma_b \gg 1$ (ultrarelativistic). In between those extrema of γ_b values, such a η expression might prove erroneous. Correct expression fulfilling relativistic kinematics should then read, in dimensionless form,

$$\frac{V_y^b}{c} = \left(\frac{\theta_y^p}{m\gamma_b} \right)^{1/2} \left(\frac{2}{\gamma_b} + \frac{\theta_y^p}{m c^2 \gamma_b} \right)^{1/2}, \\ \rightarrow \left(\frac{\theta_y^p}{m c^2 \gamma_b} \right)^{1/2}, \quad \gamma_b \gg 1, \quad (10)$$

with γ_b^\perp , Lorentz factor for beam transverse motion.

In this linear formalism, A and B [cf. Eq. (9b)] qualify positive asymmetry parameters > 1 , for target plasma and beam, respectively. They play a pivotal role in the ensuing numerical analysis, and depend on momenta

$$P_d^b = m\gamma_b V_z^b, \quad P_d^p = P_d^b \frac{n_b}{n_p \gamma_b}. \quad (11)$$

It is sufficient for FIS purposes, to restrict attention to a nonrelativistic target plasma with

$$\theta_{x,y}^p < 10 \text{ keV}.$$

In the right-hand side of Eq. (5), we use a split Krook term $\nu = \nu_p + \nu_b$. Both terms essentially document the electron-electron collision frequency [26]

$$\nu_{p,b} = 2.91 \times 10^{-6} \frac{n_{p,b}(\text{cm}^{-3})}{T_{p,b}(\text{eV})^{3/2}} \ln \Lambda_{p,b}, \quad (12a)$$

in terms of usual Coulomb logarithm. ν_p should also include a small electron-ion term $\nu_p/2.5$, so one finally gets

$$\nu_p = 3.31 \times 10^{-6} \frac{n_p(\text{cm}^{-3})}{T_p(\text{eV})^{3/2}} \ln \Lambda_p, \quad (12b)$$

$$\nu_b = 2.91 \times 10^{-6} \frac{n_b(\text{cm}^{-3})}{T_b(\text{eV})^{3/2}} \ln \Lambda_b, \quad (12c)$$

In Eqs. (12a)–(12c) one has

$$\ln \Lambda_{p,b} = \ln[9N_D],$$

with

$$N_D = \frac{1.72 \times 10^9 T_{p,b}^{3/2}(\text{eV})}{n_{p,b}^{1/2}(\text{cm}^{-3})}.$$

Target plasma is taken in thermal equilibrium ($T_e = T_i$) with $\bar{Z} = 1$ for a DT mixture.

Ion-ion collision frequency,

$$\nu_{pi} \cong \frac{2.9 \times 10^{-6}}{60} \frac{n_p(\text{cm}^{-3})}{T_p(\text{eV})^{3/2}} \ln \Lambda_p,$$

is usually negligible.

The beam-plasma model elaborated in Ref. [7] is especially appealing in a FIS context in view of its explicit dependence on density ratio n_p/n_b , and isotropic temperatures T_p and T_b , for target and REB plasma, respectively.

This choice significantly departs from several earlier investigations devoted to the electron collisional taming of the WEI [8,9,11,27]. Those latter do not stress such a marked distribution between beam and target plasmas. This point of view leads Honda [11] and Krainov [27] to endow the target plasma with relativistic properties, although its temperature should be kept under 10 keV, to motivate a FIS approach to ICF. Of course, astrophysical applications are not concerned by this remark. Even doing so, Honda [11] and Krainov [27] came up with contradictory conclusions about the estimate of the electron (beam)-ion (target) collision frequency ν_{ei} taken in a relativistic Mott setting. For instance, as soon as $n_p \geq 10^{23}$ electrons/cm³, Eq. (1) in Ref. [11] displays a normalized frequency $\nu_{ei}/\omega_p > 1$, which precludes any linear treatment of the Vlasov-Maxwell system of equations. On the other hand, we confirm Krainov [27] estimate $\nu_{ei}/\omega_p < 1$. However, we think it more appropriate to tackle FIS physics with $T_b \neq T_p$, while the choice of a unique temperature in Ref. [27] seems adequate if one restricts to photoionization of bound electrons through ultraintense lasers.

Linear dispersion relations (6)–(8) may now be easily worked out through appropriate dimensionless variables

$$x = \frac{\delta}{\omega_p}, \quad y = \frac{kc}{\omega_p},$$

$$V_1 = \frac{V_y^b}{c}, \quad V_2 = \frac{V_y^p}{c},$$

$$r = \frac{n_b}{\gamma_b n_p}, \quad n_1 = \frac{\nu_b}{\omega_b}, \quad n = \frac{\nu_p}{\omega_p}, \quad (13)$$

with $V_{1,2}$ highlighting the central significance of velocities transverse to initial beam orientation. Equations (6)–(8) now become

$$1 + (1 + [-A + (1-A)n/x][1 - 1.2533(x+n)/yV_2])/[x(x+n)] + r(1 - B[1 - 1.2533(x+n_1)/(yV_1)])/x(x+n_1) + y^2/x^2 = 0, \quad |\xi| < 1, \quad |\eta| < 1,$$

$$1 + (1 - [A + (A-1)n/x][yV_2/(n+x)]^2)/[x(x+n)] + r(1 - B[1 - 1.2533(x+n_1)/(yV_1)])/x(x+n_1) + y^2/x^2 = 0, \quad |\xi| > 1, \quad |\eta| < 1,$$

$$1 + (1 - [A(1+n/x) - n/x][1 - 1.2533(x+n)/yV_2])/[x(x+n)]r(1 - By^2V_1^2/x+n_1)/x(x+n_1) + y^2/x^2 = 0, \quad |\xi| < 1, \quad |\eta| > 1,$$

$$1 + (1 - [A + (A-1)n/x][yV_2/(x+n)]^2)/[x(x+n)] + r[1 - B(yV_1/x+n_1)^2]/x(x+n_1) + y^2/x^2 = 0, \quad |\xi| > 1, \quad |\eta| > 1. \quad (14)$$

Algebraic equations (14) are derived through standard asymptotic expansions of the dielectric function (3), given respectively as

$$W(z) = i\sqrt{\frac{\pi}{2}} Z e^{-Z^2/2} + \left(\frac{\pi}{2}\right)^{1/2} Z e^{-Z^2/2} + 1 - Z^2 + \frac{Z^4}{3} + \dots + \frac{(-)^{n+1} Z^{2n+2}}{(2n+1)!!} + \dots \quad (15)$$

for $|Z| \ll 1$ and also

$$W(z) = i\sqrt{\frac{\pi}{2}} Z e^{-Z^2/2} - \frac{1}{Z^2} - \frac{3}{Z^4} \dots \frac{(2n-1)!!}{Z^{2n}}, \quad (16)$$

for $|Z| \gg 1$.

Expansions (15) and (16) then allow to qualify the four approximations successively declined in Eq. (14) as hot-hot ($|\xi| < 1$ and $|\eta| < 1$) with $x/y < \inf(V_1, V_2)$, hot-cold ($|\xi| > 1$ and $|\eta| < 1$) with $V_2 < x/y < V_1$, cold-hot ($|\xi| < 1$ and $|\eta| > 1$) with $V_1 < x/y < V_2$, and cold-cold ($|\xi| > 1$ and $|\eta| > 1$) with $x/y > \sup(V_1, V_2)$. Dispersion relations (14) document the pertinence of transverse velocities in REB and target plasma, respectively.

IV. QUASILINEAR ANALYSIS

It is now appropriate to supplement the above linear analysis based on rectilinear trajectories of plasma particles with more realistic ones including the effects of local and self-induced electric $\vec{E}(\vec{k}, \omega)$ and magnetic $\vec{B}(\vec{k}, \omega)$ fields. This is precisely the goal of the so-called weak turbulence theory [7(a),17,18,21] initially phrased out by Dupree [17] and Weinstock [18]. Here, we use with Okada-Niu [7(a)] a convenient presentation of this theoretical framework due to Kono and Ichikawa [18]. It starts with a nonlinear dispersion relation for a purely transverse mode written as

$$1 + \chi^{\text{NL}}(k, \omega) = \frac{k^2 c^2}{\omega^2}, \quad (17)$$

with the nonlinear susceptibility

$$\chi^{\text{NL}}(\vec{k}, \omega) = \frac{4\pi e^2}{\omega} i \int d\vec{p} \vec{G}(\vec{k}, \vec{p}, \omega) \left[\left(1 - \frac{\vec{k} \cdot \vec{v}}{\omega} \right) v + \left(\frac{v^2}{\omega} - \frac{\vec{k} \cdot \vec{v}}{k^2} \right) k \right] \cdot \frac{\partial f(\vec{p})}{\partial \vec{p}}, \quad (18)$$

in terms of the Fourier transform of the particle orbit Green function including secular terms in the form

$$\vec{G}(k, v, \omega) = \int_0^\infty dt \exp \left[i(\omega - \vec{k} \cdot \vec{v})t - \frac{1}{3} \vec{D}(\vec{v}) k^2 t^3 \right], \quad (19)$$

where

$$\vec{D}(\vec{v}) = \frac{e^2}{(m\gamma_b)^2} \sum_{\vec{k}_1} \int \frac{d\omega_1}{2\pi} \left| \vec{E}(\vec{k}_1, \omega_1) + \frac{\vec{v}}{c} \times \vec{B}(\vec{k}_1, \omega_1) \right|^2 \times \int_0^\infty dt \exp \left[-i(\omega_1 - \vec{k}_1 \cdot \vec{v})t - \frac{1}{3} \vec{D}(\vec{v}) k_1^2 t^3 \right] \quad (20)$$

denotes a self-consistent, velocity-dependent and renormalized diffusion coefficient including the influence of local electric and magnetic fields on particle trajectories.

At this juncture it proves convenient to introduce a vertex function $\Gamma(k, v)$ through

$$\Gamma^3(k, v) = k^2 \vec{D}(v), \quad (21)$$

which allows approximating $\text{Im}(\chi^{\text{NL}})$ with

$$\text{Im} \left\{ \chi^{\text{NL}} \left(\frac{\theta_y^p}{m}, \frac{\theta_y^b}{m\gamma_b} \right) \right\} \cong \text{Im} \left\{ \chi^L \left(\frac{\theta_y^p}{m} + \frac{\Gamma^2(k, v_c)}{k^2}, \frac{\theta_y^b}{m\gamma_b} + \frac{\Gamma^2(k, v_c)}{k^2} \right) \right\}, \quad (22)$$

and

$$\text{Re}(\chi^{\text{NL}}) \cong \text{Re}(\chi^L), \quad (23)$$

where v_c is the critical velocity [28] given by

$$(\omega - kv_c)^2 \cong 2\Gamma(k, v_c)^2. \quad (24)$$

The nonlinear saturation level can be derived from the vanishing of nonlinear growth rate of unstable waves at saturation, i.e.,

$$\text{Im}(1 + \chi^{\text{NL}}) = 0. \quad (25)$$

By using Eqs. (22), (24), and (25), the saturation value of $\Gamma(k, v_c)$ can be determined as the largest solution of the bi-quartic equation:

$$\left(1 + \frac{\omega_b^2}{\omega_p^2} \right) \Gamma^4(k, v_c) - \left[\frac{\omega_b^2 p_d^{b2}}{\omega_p^2 (m\gamma_b)^2} + \frac{\theta_x^p}{m} + \frac{p_d^{p2}}{m^2} - \left(1 + \frac{\omega_b^2}{\omega_p^2} \right) \times \left(\frac{\theta_y^p}{m} + \frac{\theta_y^b}{m\gamma_b} \right) \right] \Gamma^2(k, v_c) k^2 - \left[\frac{\omega_b^2 p_d^{b2}}{\omega_p^2 (m\gamma_b)^2} + \frac{\theta_y^p}{m} + \left(\frac{\theta_x^p}{m^2} + \frac{p_d^{p2}}{m^2} \right) \frac{\theta_y^p}{m} - \left(1 + \frac{\omega_b^2}{\omega_p^2} \right) \frac{\theta_y^p \theta_y^b}{m m\gamma_b} \right] k^4 = 0. \quad (26)$$

Denoting such a solution as $\chi = \Gamma(k, v_c)/k$ and expliciting the equivalences

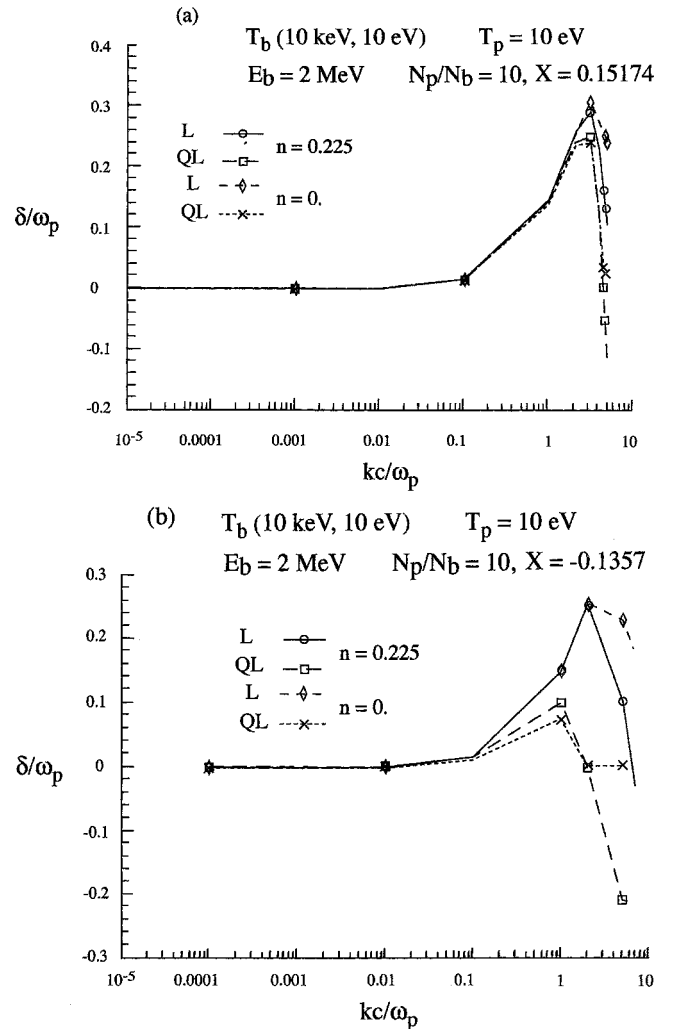


FIG. 2. WEI growth rates in terms of wave number for a hot REB ($\theta_y^p = 10$ keV, $\theta_x^p = 10$ eV) impinging a cold plasma with $n_p/n_b = 10$ and ($\theta_y^b = \theta_x^b = 10$ eV). (a) A' and B' [Eq. (28)] with the largest root of Eq. (26). (b) A' and B' with the next largest root of Eq. (26). $n_b = 10^{22}$ e cm $^{-3}$.

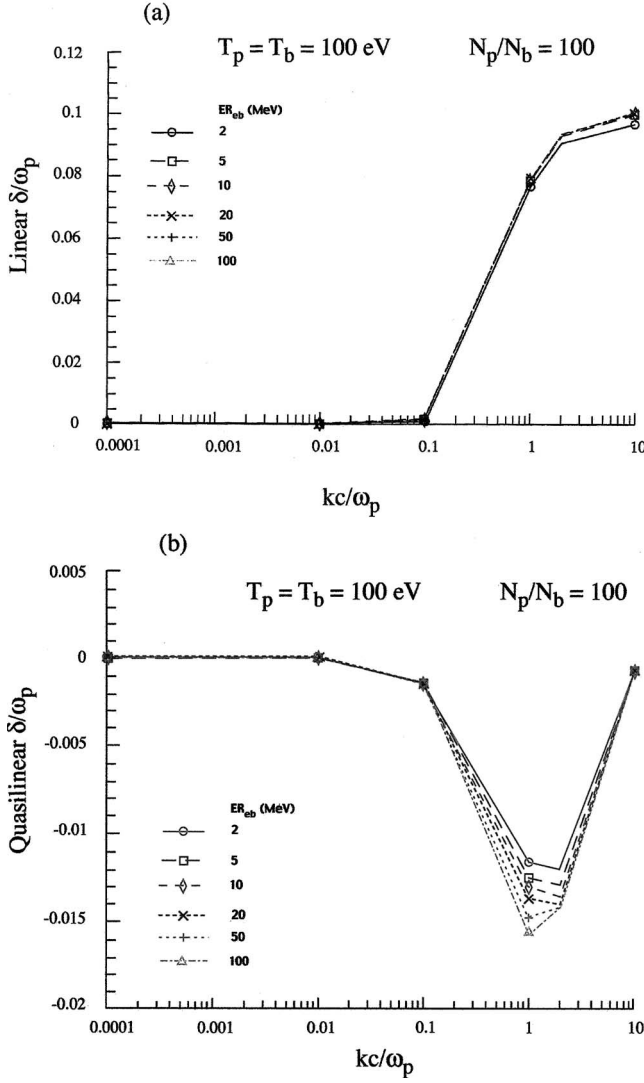


FIG. 3. WEI GR profiles with $T_p = T_b = 100$ eV and $n_p/n_b = 100$ with projectile energy $E_b \in [2, 100]$ keV. (a) Linear (L) growth rates. (b) Quasilinear (QL) growth rates $n \neq 0$ and $n_1 \neq 0$.

$$\theta_y^p/m \rightarrow \theta_y^p/m + \frac{\omega_b^2 p_d^{b2}}{\omega_p^2 m^2 \gamma_b^2}, \quad (27a)$$

$$\theta_y^p/m\gamma \rightarrow \theta_y^p/m\gamma + \frac{\omega_b^2 p_d^{b2}}{\omega_p^2 m^2 \gamma_b^2}, \quad (27b)$$

with $p_d^b = mV_b\gamma_b$ validating Eqs. (22) and (23), one is led to replace asymmetrical parameters A and B given in Eq. (9b) with

$$A' = \frac{AT_p}{T_p + XD}, \quad B' = \frac{BT_b}{T_b + XD}, \quad (28)$$

and $D = 511r(1 - \gamma_b^{-2})$. T_p and T_b being evaluated in keV. One should also notice that the other and disregarded solutions of Eq. (26) lead to an even lower saturation level. So, by sticking to the highest and positive solution, we indeed minimize the considered saturation level, and corresponding reduction of the WEI growth rate. A significant illustration of such an

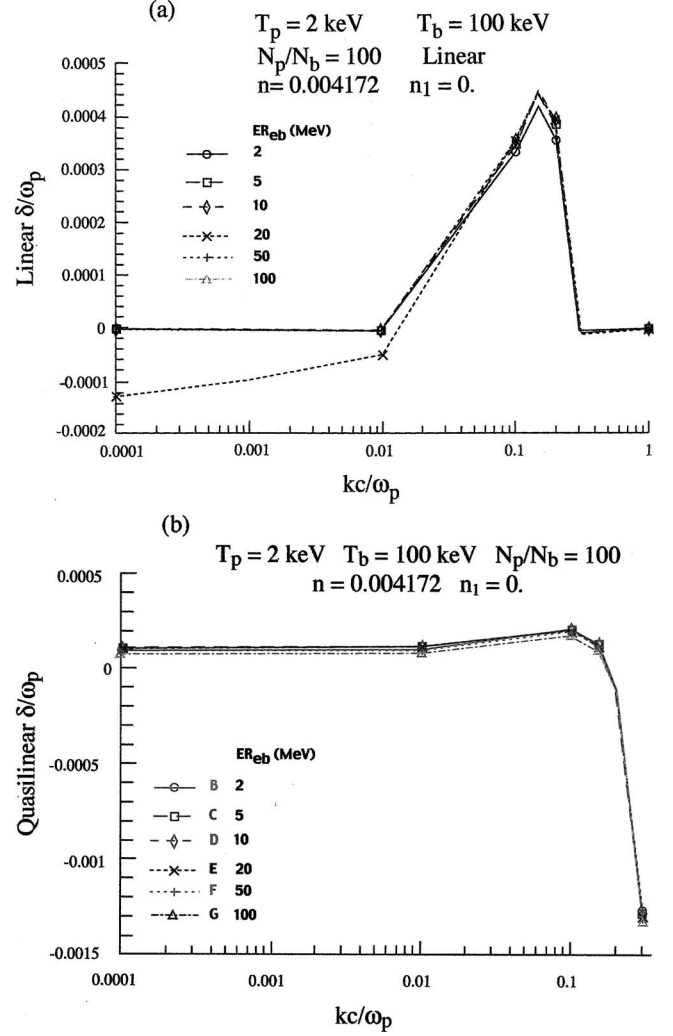


FIG. 4. Same caption as Fig. 3 with $T_p = 2$ keV, other parameters unchanged. (a) L with $n \neq 0$ and $n_1 \neq 0$. (b) QL with $n \neq 0$ and $n_1 = 0$.

approach is given in Fig. 2 with a hot 2 MeV REB and a strongly anisotropic thermal distribution ($\theta_y^b = 10$ keV, $\theta_x^b = 10$ eV) interacting with a rather cold plasma target ($\theta_y^p = \theta_x^p = 100$ eV), ten times more dense than the incoming beam. The two considered roots of Eq. (28) are significantly different, while corresponding growth rate profiles look rather similar. Indeed the largest X value features slighter lower δ than these pertaining to the next X value.

V. WEI GROWTH RATES (GR) PROFILES

In such investigations much of the relevant physics is unravelled by profiles of WEI growth rates normalized with target plasma frequency ω_p in terms of dimensionless wave number kc/ω_p scaled by the inverse of target skin depth.

Using respectively (A, B) and (A', B') [Eqs. (27a) and (27b)] into the relevant linear dispersion relations (14), we obtain the WEI growth rates depicted as linear (L) and quasilinear (QL), respectively.

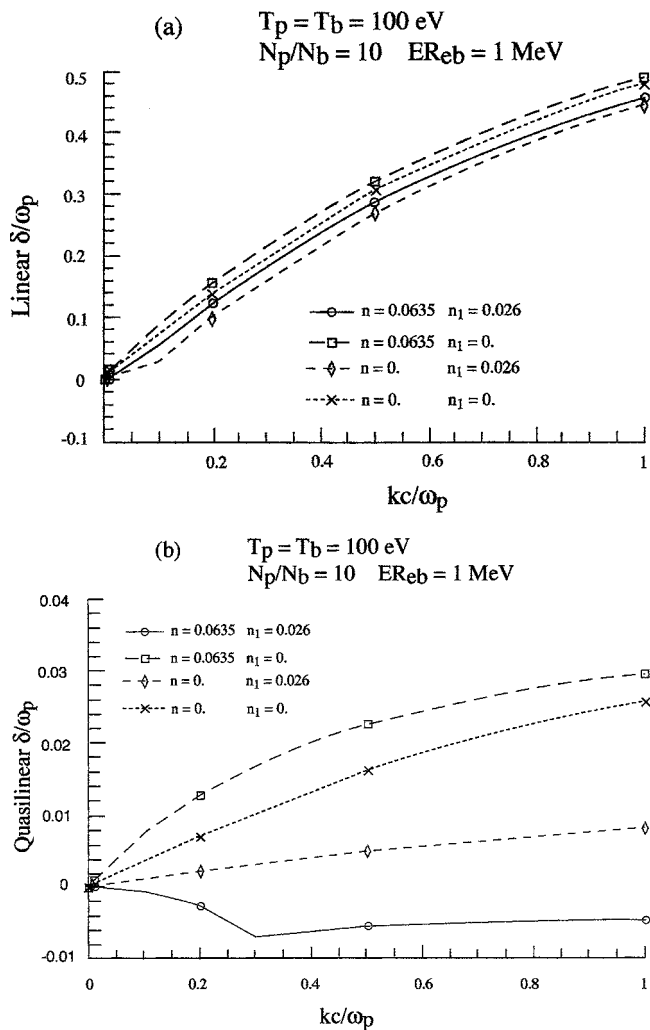


FIG. 5. WEI GR profiles with $T_p=T_b=100 \text{ eV}$, $n_p/n_b=10$, and $E_b=1 \text{ MeV}$ in terms of n and n_1 . (a) L; (b) QL.

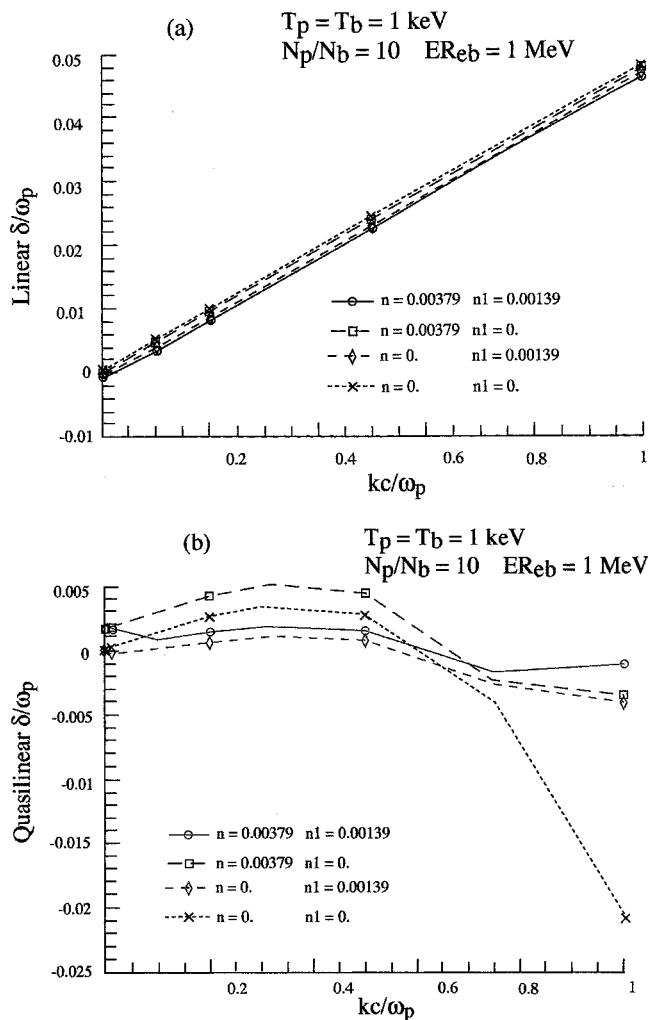


FIG. 7. Same caption as Fig. 5 with $T_p=T_b=1 \text{ keV}$.

A. Basic trends

Recalling that the best performing FIS scenarios demand a nearly isentropic precompression with as low as possible a target temperature T_p . We consider in Fig. 3 a typical REB-plasma system with also a cold beam ($T_b=100 \text{ eV}$) for a density ratio $n_p/n_b=100$, already achieved in some preliminary, and low energy scale experiments [29] with ultraintense petawatt (PW) lasers. Figure 3(a) features linear (L) GR parametrized for several REB energies, and steadily increasing for $0.1 \leq kc/\omega_p \leq 10$. Beam energy dependence appears nearly negligible. Those outputs display a marked contrast with their quasilinear (QL) counterparts, which remain always negative with a conspicuous dip replacing former positive slop. In both cases (L and QL) collisions with $n \neq 0$ and $n_1 \neq 0$ are retained in target plasma and REB, as well. Main provisional conclusion displayed by these captions is a significant QL stabilizing effect. Switching now to a higher target temperature with $T_p=2 \text{ keV}$ in Fig. 4, for a much higher beam temperature ($T_p=100 \text{ keV}$), we have now $n_1 \cong 0$. Then, one witnesses an overall behavior quite similar to former one with quasinegligible GR in the $n \neq 0$ quasilinear approximation. Again REB energy dependence is hardly noticeable.

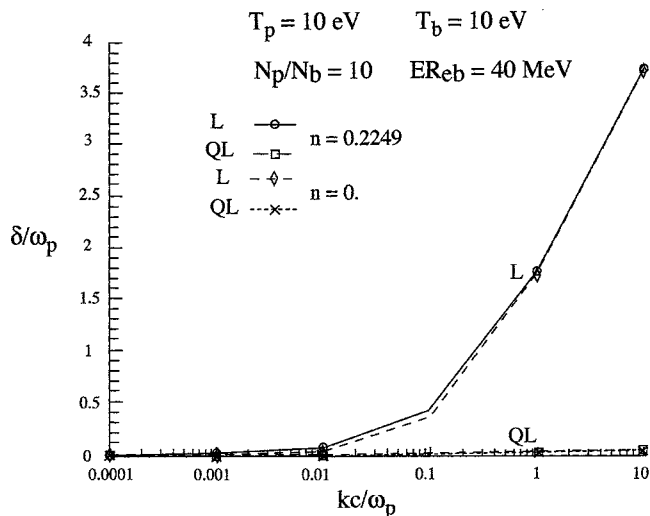


FIG. 6. WEI GR profiles with $T_p=T_b=10 \text{ eV}$, $n_p/n_b=10$, and $E_b=40 \text{ MeV}$. $n_1=0$.

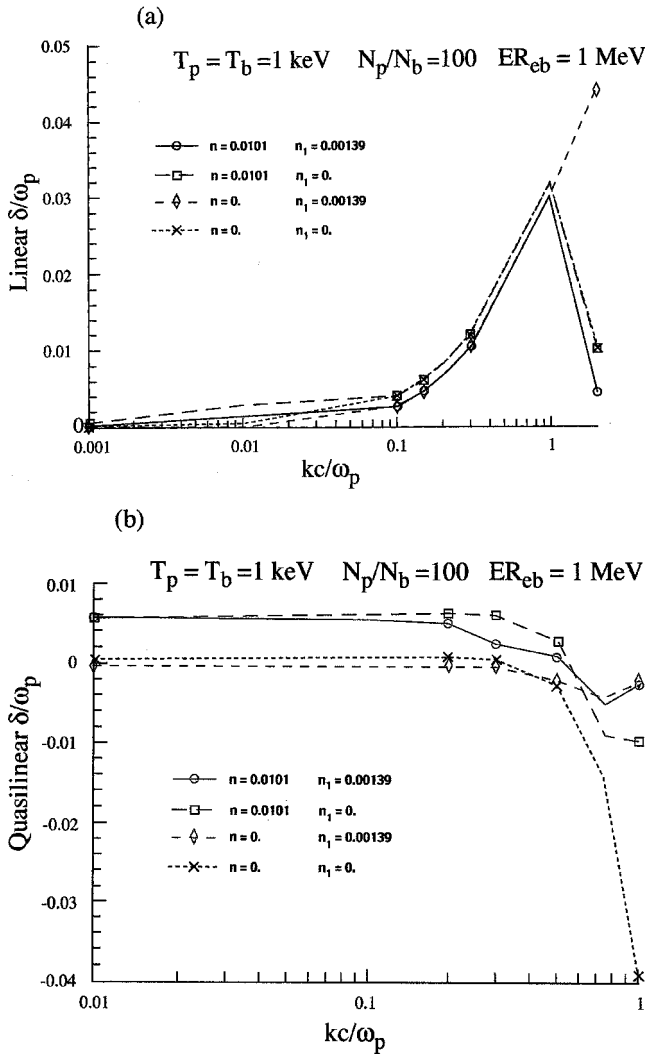


FIG. 8. Same caption as Fig. 7 with $n_p/n_b=100$.

Switching now to a low density ratio $n_p/n_b=10$ (Fig. 5) for a cold beam-target system makes to appear a subtle interplay of QL and collision effects. First, the latter are seen to have a rather small impact on the L profiles [Fig. 5(a)], while QL ones [Fig. 5(b)] are strongly affected. $n \neq 0$ and $n_1 \neq 0$ are shown to yield a negative δ profile for all $kc/\omega_p \leq 1$. Profile with $n \neq 0$ and $n_1=0$ confirms a previous finding [8,9,30] documenting enhanced values above collisionless ones, with further damping to negative values as soon as $kc/\omega_p > 1$ (not shown on Fig. 5).

On the other hand, considering high projectile energy $E_b=40$ MeV (Fig. 6) confirms QL stabilizing effect altogether with a negligible of beam-target collision contribution ($n \neq 0$) when $n_1=0$.

It is also rather instructive to mention global trends showed by linear and quasilinear growth rates. The most conspicuous one features a very small linear-quasilinear discrepancy at large beam temperature $T_b \geq 300$ keV, valid for all r, T_p and kc/ω_p values.

A more obvious one involves the merging of linear and quasilinear growth rates at large wavelength fulfilling $kc/\omega_p \leq 0.01$.

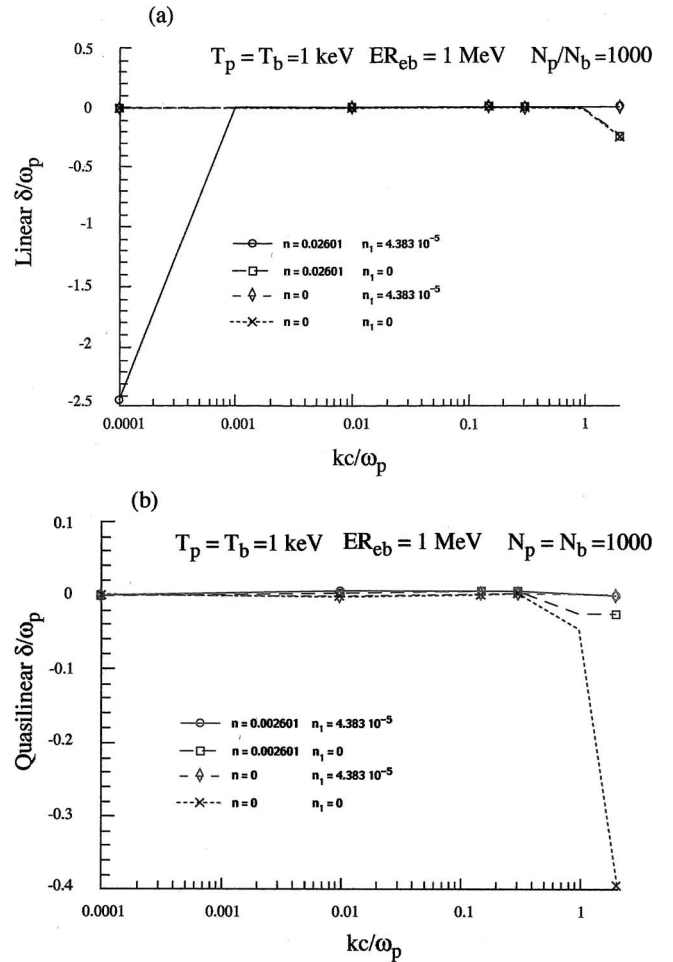


FIG. 9. Same caption as Fig. 7 with $n_p/n_b=1000$.

B. n_p/n_b dependence

Figures 7–10 illustrate a typical beam-target interaction with $T_p=T_b=1$ keV and $E_b=1$ MeV with n_p/n_b ranging from 10 up to 10^4 . Significant qualitative and quantitative discrepancies remain noticeable for $n_p/n_b \leq 100$. At higher density ratio, L and QL profiles exhibit full stabilization, which thus highlights the basic soundness of the wedged-cone approach to fast ignition [29] with REB directly introduced close to the dense core. Also the $n \neq 0$ and $n_1 \neq 0$ profile, albeit on the $\delta/\omega_p=0$ line, remains the highest, for L—as well as for the QL—approximation. It should be recalled that maintaining T_p constant while rising n_p keeps n increasing too, while decreasing n_1 . The $n_p/n_b=10$ (Fig. 7) case is particularly instructive, in this regard.

Linear GR are seen monotonously increasing for any collisionality n (target) or n_1 (beam) in the whole wavelength range. Quasilinear GR turn negative as soon as $kc/\omega_p \geq 0.6$. It has to be noticed that retaining collisions only in target plasma enhance GR at $kc/\omega_p \leq 0.6$, while restricting them to beam plasma produces the lowest GR. Keeping them in target and beam plasmas still constrain the growth rate within acceptable values for permitting an efficient target ignition through beam collisional stopping.

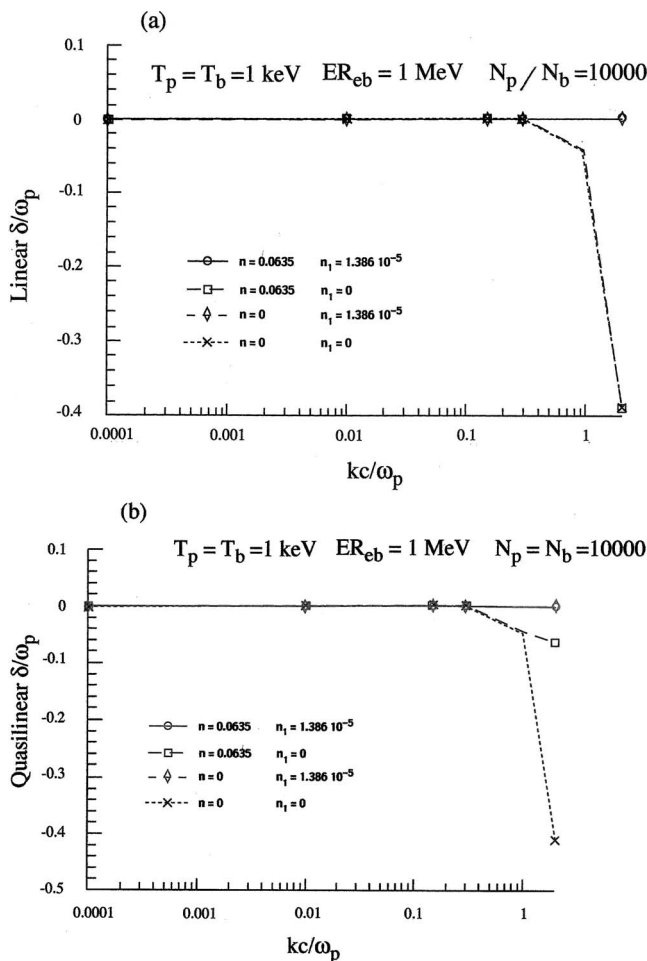


FIG. 10. Same caption as Fig. 7 with $n_p/n_b=10000$.

It is also of a certain interest to check the n_p/n_b dependence at higher target temperature. Figure 11 exhibit corresponding variations for $T_p=10$ keV, $T_b=1$ keV, $E_b=1$ MeV, and $n \neq 0$ with vanishing n_1 . One can thus witness that a high T_p target features a WEI-immune beam-target interaction. L and QL profiles remain always stable, for all n_p/n_b ratio. Unfortunately, FIS [1] is mostly efficient for $T_p \leq 1$ keV, where WEI growth rates demand a clever taming.

C. High beam temperature

Now, we switch attention to REB-target plasma interaction with an isotropic beam temperature $T_b \geq 100$ keV, in order to investigate the resulting potential for WEI taming.

First it should be noticed that whatever the longitudinal beam temperature T_b^{\parallel} is, the joint distribution (4) delivers GR values independent of T_b^{\parallel} .

First, we pay attention to rather cold targets with $T_p = 100$ eV so that $n \gg n_1$, which could allow to neglect n_1 .

Figure 12 feature corresponding GR profiles with $T_b = 500$ keV and 1 MeV, respectively for $n_p/n_b=100$ and $E_b = 5$ MeV. Figure 12(a) demonstrates a strong collision (4) effect with identical L and QL results. The $n \neq 0$ profile again confirms a behavior noticed several times previously [8,9,30]. WEI δ values for $kc/\omega_p < 1$ get enhanced with re-

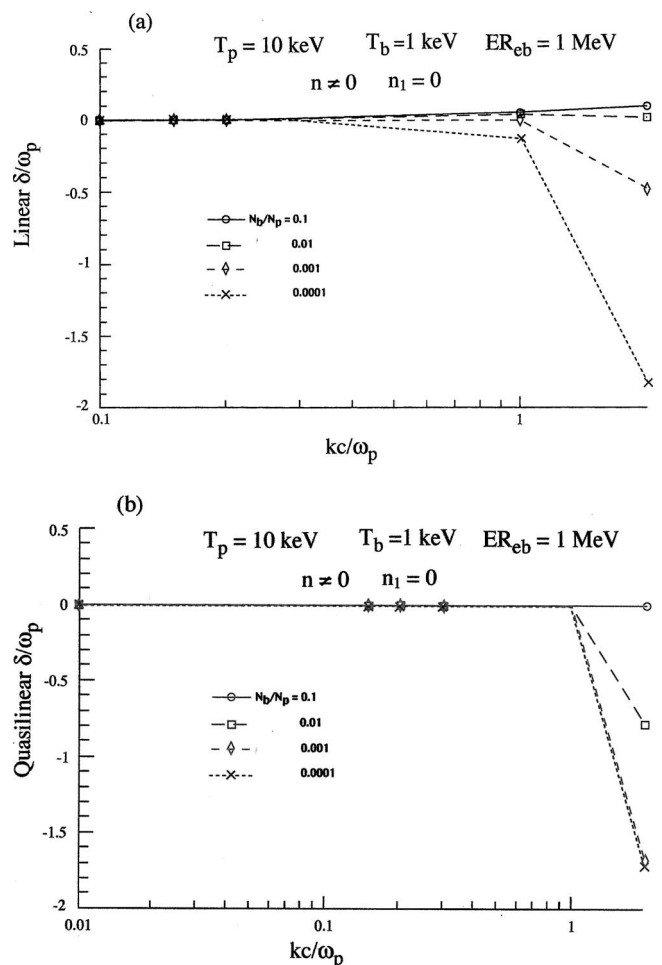


FIG. 11. WEI GR profiles with $T_p=10$ keV, $T_b=1$ keV, $E_b = 1$ MeV, $n \neq 0$, and $n_1 \neq 0$, in terms of density ratio n_p/n_b . (a) L; (b) QL.

spect to collisionless ones, and drop to negative (damping) values for $kc/\omega_p \geq 0.4$. A factor of 2 increase in plasma temperature produces flat L as well as QL profiles [Fig. 12(b)]. Moreover, in agreement with above results, they remain unchanged in the E_b range 5–50 MeV.

Keeping same T_b values in the 0.5–1 MeV range while increasing T_p and n_p/n_b [Fig. 13(a)] or T_p and E_b [Fig. 13(b)] simplify greatly the GR profiles. Linear-quasilinear differences practically disappear as well as $n \neq 0$ enhancement effect for $kc/\omega_p < 1$.

Increasing significantly the target plasma density and the beam temperature (Fig. 13) renders negligible the intrabeam collision term fulfilling now $n_1 \ll n$. The very high T_b value, in MeV range erases very efficiently any positive growth rate, thus featuring a beam-target interaction stable at any plasma wave number k .

These preliminary results highlight again the cone-angle scenario [29,6] with laser produced electrons close to highest density core in the precompressed DT fuel.

Another figure of merit illustrating the stabilizing effect of beam temperature, especially the transverse one, is the maximum wave number k_{\max} yielding a non-negative growth rate

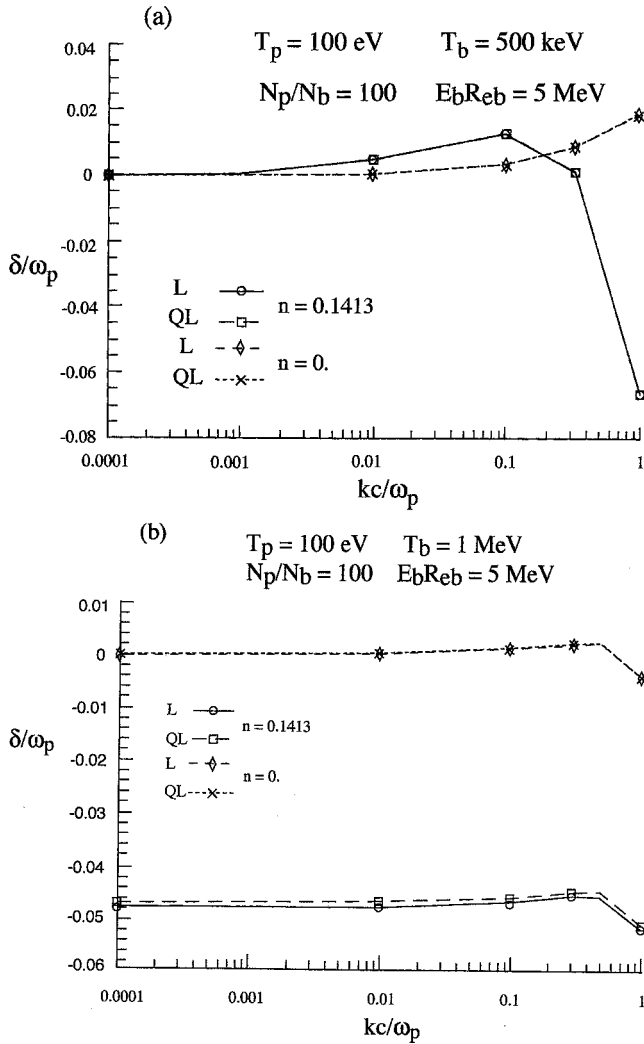


FIG. 12. WEI GR profiles at high T_b with $T_p=100$ eV, $n_p/n_b=100$, and $E_b=5$ MeV. $n \neq 0$ and $n_1=0$. (a) $T_b=500$ keV; (b) $T_b=1$ MeV.

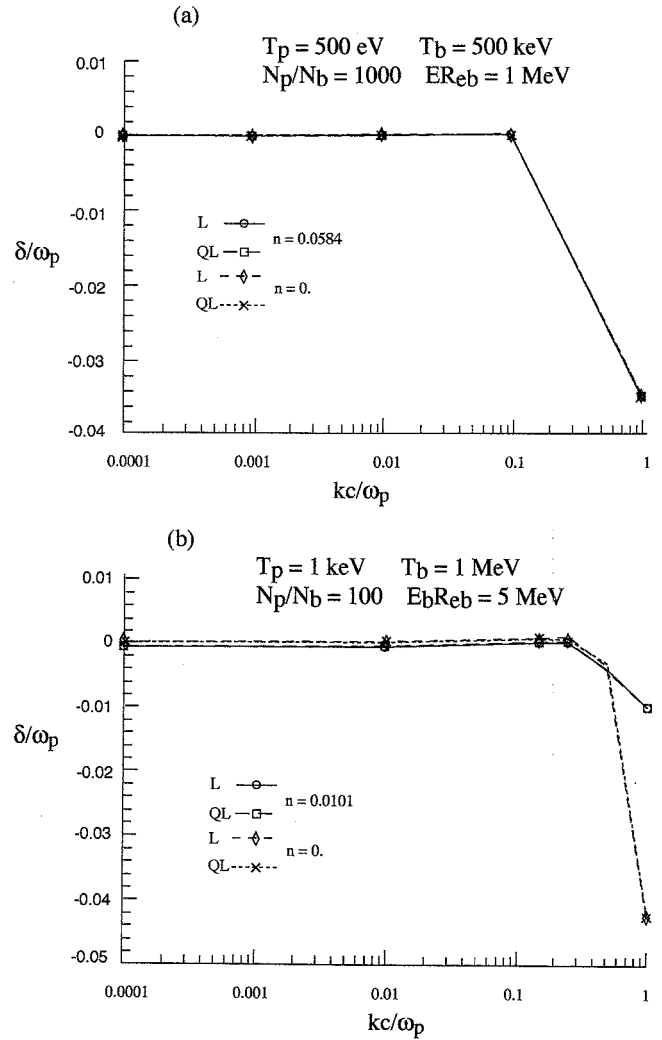


FIG. 13. WEI GR profiles at high T_b . (a) $T_p=500$ eV; $T_b=500$ keV; $n_p/n_b=10^3$; $E_b=1$ MeV. (b) $T_p=1$ keV; $T_b=1$ MeV; $n_p/n_b=100$; $E_b=5$ MeV.

(Fig. 14). Here we selected a target plasma with parameters close to those of the Osaka experiment [29], with $T_p=100$ eV and $n_p/n_b=100$ so that $n=0.1413$.

k_{max} is then seen steadily decreasing as T_b increases. We already noticed that isotropic and transverse T_b gives identical growth rates, in the present formalism. Recently, an alternative approach to FIS has been advocated by Malkin and Fisch [31] through highly energetic REB for controlling the onset of Langmuir waves, thus featuring an ultimate and nonlinear stage of WEI development. In Fig. 15, we probe these suggestions with a target density $n_p \sim 10^{26}$ electrons/cm³ and a 100 MeV REB. Such a beam is likely to have a beam energy spread (T_b) at least of the order of 100 keV. Corresponding Weibel instability does not appear damaging for this situation. So, the given scheme [31] could retain some credence in FIS context.

Finally, it appears of interest to notice that in the hot beam-hot target option of concern in many FIS situations the maximum growth rate could be well approximated by [7(b)]

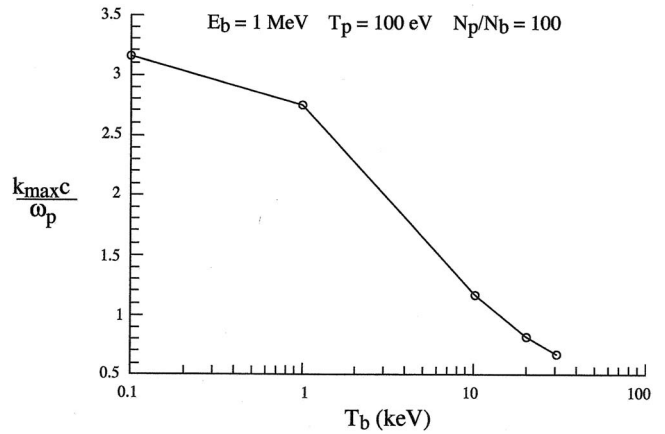


FIG. 14. Maximum wave number for positive growth rate in terms of REB temperature.

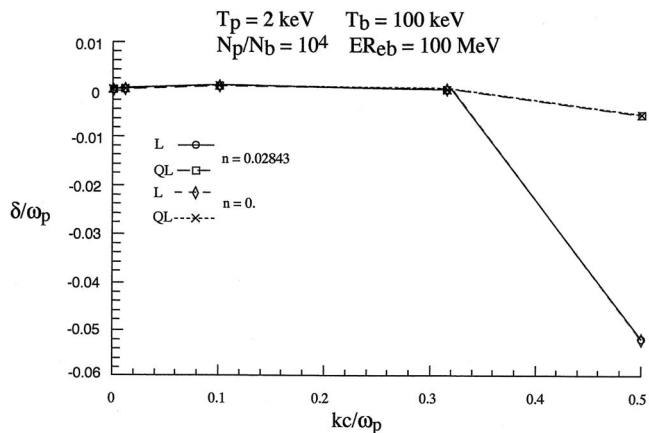


FIG. 15. WEI GR profiles with $E_b=100$ MeV and $T_b=100$ keV in a dense core with $n_p/n_b=10^4$ and $T_p=2$ keV.

$$\delta_{\max} = \left(\frac{8}{27\pi}\right)^{1/2} \frac{\omega_p}{c} \left[(A-1) + (B-1) \frac{\omega_b^2}{\omega_p^2} \right]^{1/2} \left[\frac{A}{v_y^p} + \frac{B}{v_y^b} \frac{\omega_b^2}{\omega_p^2} \right]^{-1} - \frac{\nu}{v_y^p} (A-1) \left[\frac{A}{v_y^p} + \frac{B}{v_y^b} \frac{\omega_b^2}{\omega_p^2} \right]^{-1}, \quad (29)$$

at

$$k_{\max}^2 = \frac{1}{3} \frac{\omega_p^2}{c^2} \left[(A-1) + (B-1) \frac{\omega_b^2}{\omega_p^2} \right], \quad (30)$$

ν -independent locations. L and QL values are respectively obtained through (A, B) from Eqs. (9b) and (28).

VI. CONCLUSIONS

We thoroughly explored every possible extension of the linear Vlasov-Maxwell formalism [7] for the excitation of electromagnetic collective modes in the interaction of intense relativistic electron beams (REB) with a density gradient of supercompressed deuterium+tritium (DT) fuel. We first witnessed a highly encouraging feature of the quasilinear (QL) growth rates which appear strongly damped with respect to their purely linear (L) counterparts, except when both show up negative.

We also investigated at length electron-electron collisions between REB and target plasmas (T_p) as well as within incoming REB plasma. We found that QL growth rates are often more affected by collisions than linear ones. This latter appreciation has to be nuanced, as follows. Restricting to REB-target plasma collisions, with $n \neq 0$ and $n_1=0$, one essentially confirms a behavior documented previously [8,9,31] according to which δ gets enhanced above collisionless values ($n=0$, $n_1=0$) as long as $kc/\omega_p < 1$. On the other hand, as soon as $kc/\omega_p \geq 1$, collisions drive the growth rates

to negative values. The inclusion of intra-REB scattering does accentuate such a trend for a cold beam-cold T_p interaction [see, for instance, Fig. 5(b)].

However, enhanced beam and target temperatures [see Fig. 7(b)] could also produce, at $kc/\omega_p \geq 1$, δ/ω_p values larger than collisionless ones.

Such conflicting behaviors induced us to consider with attention the damping of WEI growth rates through significant reduction of density ratio n_b/n_p or rather high beam temperature T_b . It should be appreciated that in the course of these investigations a certain attention to moderate T_p has been paid in the 100 eV–1 keV range, in order to cope with the fast ignition scenario (FIS) in its most promising cone-angle configuration with $n_b/n_p \geq 100$ [29].

Our studies clearly demonstrate that giving a due attention to distinct REB and T_p temperatures could provide an efficient tuning of the WEI growth rate profiles.

Finally, it remains to perform a systematic investigation of nonlinear WEI growth rates.

Indulging now into a more global perspective, one could wonder about further refinements of growth rate calculations, beyond the present quasilinear formalism. A preliminary step in this direction could involve a 3-wave interaction mechanism. However, the numerous and very intense PIC simulations devoted to the fully nonlinear regime obviously demand a more ambitious theoretical framework. Despite that such a framework is not yet available, one could speculate that present quasilinear improvements have only the status of higher order corrections to an initial asymptotic approximation to the complete nonlinear growth rate. In such an occurrence, it appears problematic to bridge straightforwardly the wide gap between present quasilinear treatment and a fully nonlinear one.

Presently, it appears much more profitable to enlarge the linear approximation by superimposing three electromagnetic instabilities: Weibel, filamentation and 2-stream [4,32] while allowing the wave-number vector \vec{k} to take any orientation. Such an approach demonstrates that maximum growth rates appear on an oblique ridge between transverse and parallel directions with respect to the initial beam. It seems to us that quasilinear corrections to this combined approach of electromagnetic instabilities might be worthwhile to pursue.

ACKNOWLEDGMENTS

In the course of this work we derived great benefits through very stimulating intercourses with many distinguished experts including F. Califano, B. Coppi, Y. Elskens, B. Langdon, B. Lassinski, D.C. Montgomery, W. Mori, F. Pegoraro, D. Pesme, H. Ruhl, and V. Tikonchuk. This work has been partially supported under project FTN2003-00721 of the Spanish Ministerio de Education y Ciencia.

- [1] M. Tabak, J. Hammer, M. E. Glinksy, W. L. Kruer, S. C. Wilks, J. Woodworth, E. M. Campbell, M. D. Perry, and R. J. Mason, *Phys. Plasmas* **1**, 626 (1994).
- [2] See, for instance, M. V. Goldman, *Rev. Mod. Phys.* **56**, 709 (1984); P. A. Robinson, *ibid.* **69**, 507 (1997); and also R. A. Fonseca *et al.*, *Phys. Plasmas* **10**, 1979 (2003).
- [3] L. N. Vyacheslavov *et al.*, *Plasma Phys. Controlled Fusion* **44**, B279 (2002); and also *JETP Lett.* **75**, 41 (2002).
- [4] A. Bret, M. C. Firpo, and C. Deutsch, *Phys. Rev. E* **70**, 046406 (2004); *Phys. Rev. Lett.* **94**, 115002 (2005).
- [5] S. Atzeni, *Phys. Plasmas* **6**, 3316 (1999).
- [6] C. Deutsch, *Eur. Phys. J.: Appl. Phys.* **24**, 95 (2003).
- [7] T. Okada and K. Niu, *J. Plasma Phys.* **23** 423 (1980); **24**, 483 (1980).
- [8] J. M. Wallace, J. U. Brackbill, C. W. Cranfill, D. W. Forslund, and R. J. Mason, *Phys. Fluids* **30**, 1085 (1987).
- [9] W. Kruer, S. Wilks, B. Lasinski, B. Langdon, R. Town, and M. Tabak, *Bull. Am. Phys. Soc.* **48**, 81 (2003).
- [10] Z. Zinamon, E. Nardi, and E. Peleg, *Phys. Rev. Lett.* **34**, 1262 (1975).
- [11] M. Honda, *Phys. Rev. E* **69**, 016401 (2004).
- [12] F. Califano, F. Pegoraro, and S. V. Bulanov, *Phys. Rev. E* **56**, 963 (1997).
- [13] F. Califano, F. Pegoraro, S. V. Bulanov, and A. Mangeney, *Phys. Rev. E* **57**, 7048 (1998).
- [14] F. Califano, F. Pegoraro, and S. V. Bulanov, *Phys. Rev. E* **58**, 7837 (1998).
- [15] E. G. Weibel, *Phys. Rev. Lett.* **2**, 83 (1959).
- [16] H. Ruhl, *Plasma Sources Sci. Technol.* **11**, A154 (2002).
- [17] T. Dupree, *Phys. Fluids* **9**, 1773 (1966); J. Weinstock, *ibid.* **12**, 1045 (1969).
- [18] M. Kono and Y. H. Ichikawa, *Prog. Theor. Phys.* **49**, 754 (1973).
- [19] A. Ramani and G. Laval, *Phys. Fluids* **21**, 980 (1978).
- [20] G. Kalman, C. Montes, and D. Quemada, *Phys. Fluids* **11**, 1797 (1968).
- [21] R. C. Davidson, *Methods in Nonlinear Plasma Physics* (Academic Press, New York, 1972), p. 65.
- [22] R. C. Davidson, D. A. Hammer, I. Haber, and C. E. Wagner, *Phys. Fluids* **15**, 317 (1972).
- [23] Y. Elskens (private communication).
- [24] B. D. Fried and S. D. Conte, *The Plasma Dispersion Function* (Academic Press, New York, 1961), p. 1.
- [25] C. Gouedard and C. Deutsch, *J. Math. Phys.* **19**, 32 (1978), also K. V. Starikov and C. Deutsch, *Phys. Rev. E* **71**, 026407 (2005).
- [26] J. D. Huba, *NRL Plasma Formulary* (Naval Research Laboratory, Washington D.C., 1994), p. 28; S. Braginski, *Reviews of Plasma Physics* (Wiley Interscience, New York, 1965), p. 215.
- [27] V. P. Krainov, *J. Phys. B* **36**, 3187 (2003).
- [28] A. Sleeper, J. Weinstock, and B. Bezzerides, *Phys. Rev. Lett.* **29**, 343 (1972).
- [29] R. Kodama *et al.*, *Nature* **412**, 798 (2001).
- [30] C. Deutsch, *Laser Part. Beams* **22**, 115 (2004).
- [31] V. M. Malkin and N. J. Fisch, *Phys. Rev. Lett.* **89**, 125004 (2002).
- [32] A. Bret and C. Deutsch, *Phys. Plasmas* (to be published).